Lawrence Berkeley National Laboratory

Lawrence Berkeley National Laboratory

Title

Design Study of Longitudinal Dynamics of the Drive Beam in a Relativistic Klystron Two-Beam Accelerator

Permalink

https://escholarship.org/uc/item/7800g1pq

Author

Li, H.

Publication Date

2008-09-18

Lawrence Berkeley Laboratory

UNIVERSITY OF CALIFORNIA

Accelerator & Fusion Research Division

Design Study of Longitudinal Dynamics of the Drive Beam in a Relativistic Klystron Two-Beam Accelerator

H. Li, S.S. Yu, and A. Sessler

October 1994
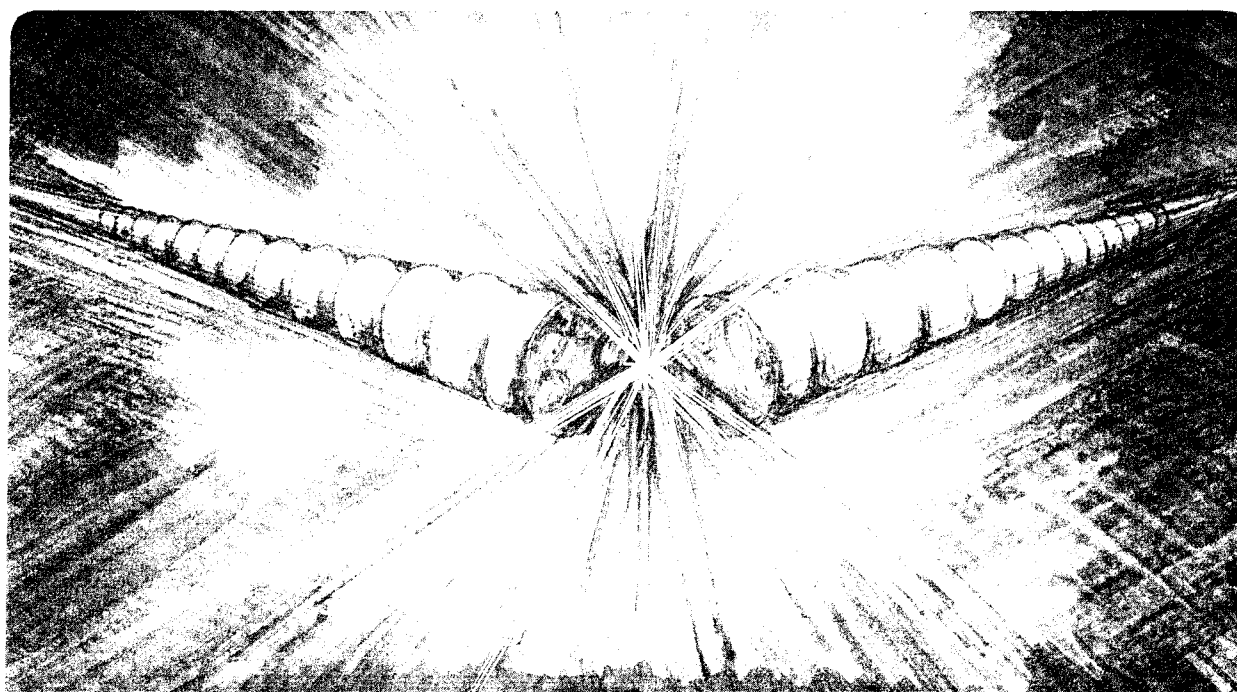
Design Study of Longitudinal Dynamics of the Drive Beam in 1 TeV Relativistic Klystron Two-Beam Accelerator*

Hai Li, Simon S. Yu and Andrew M. Sessler

Lawrence Berkeley Laboratory
University of California, Berkeley, California 94720

Abstract

In this paper we present a design study on the longitudinal dynamics of a relativistic klystron two-beam accelerator (RK-TBA) scheme which has been proposed as a power source candidate for a 1 TeV next linear collider (NLC). We address the issue of maintaining stable power output at desired level for a 300-m long TBA with 150 extraction cavities and present our simulation results to demonstrate that it can be achieved by inductively detuning the extraction cavities to counter the space charge debunching effect on the drive beam. We then carry out simulation study to show that the beam bunches desired by the RK-TBA can be efficiently obtained by first chopping an initially uniform beam of low energy into a train of beam bunches with modest longitudinal dimension and then using the "adiabatic capture" scheme to bunch and accelerate these beam bunches into tight bunches at the operating energy of the drive beam. We have also examined the "after burner" scheme which is implemented in our RK-TBA design for efficiency enhancement.

1. Introduction

Studies have been carried out on the feasibility of the concept of a relativistic klystron two-beam accelerator (RK-TBA) as a possible future linear collider because of its potential high beam to rf efficiency for the drive beam [1-11]. In a RK-TBA, one beam line is a high-gradient rf linac which accelerates e^- or e^+ to very high energies. The second beam line, the subject of this paper, consists of an induction linac and microwave generating structures that are located at regular intervals along the beam line. A schematic of the RK-TBA scheme is given in Figure 1. In contrast to conventional klystron driven linear colliders the electron beam in the second beam line of the RK-TBA drives multiple RK extraction cavities with reacceleration from induction cells between adjacent cavities, and therefore, the beam to rf conversion can be significantly increased.
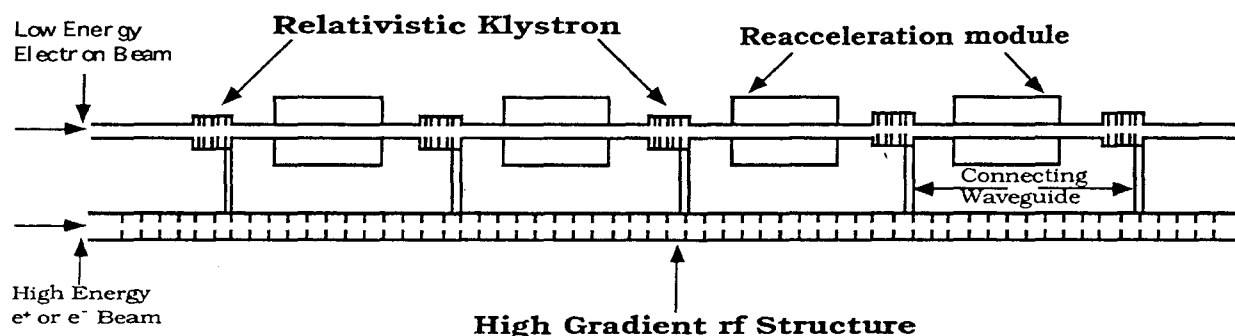

Fig. 1. Schematic of RK-TBA scheme

This work is part of a joint effort between Lawrence Berkeley Laboratory (LBL) and Lawrence Livermore National Laboratory (LLNL), which aims at achieving an overall conceptual design of a high efficiency and low cost 1 TeV RK-TBA for the next linear collider (NLC) [12]. According to our preliminary design configuration [12], the power source for a 1 TeV NLC should consist of 50 identical TBA units with 25 on each arm. A layout of one RK-TBA unit is given in Figure 2 in which, it is seen that, the injector, the chopper and the "adiabatic capture" sections comprise the front part of the TBA unit. In the main TBA section the beam undergoes many repetitions of energy extraction at the RK cavities and reacceleration along the drift tubes.
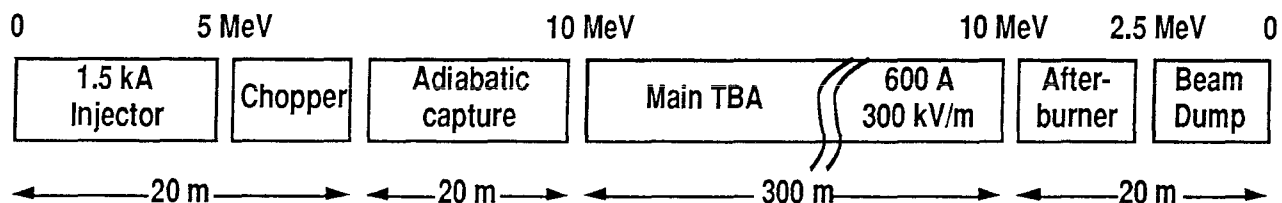

Fig. 2. Layout of one RK-TBA unit

After the beam exits the main TBA it enters the rear part of the TBA unit which consists of the "after-burner" section for further energy extraction from the beam and the beam dump section for disposing the spent beam. The design parameters of the TeV RK-TBA are based on the latest parameters of a 1 TeV linear collider considered by SLAC [13]. The principal parameters are given in Table 1. According to Table 1 the required power is about 360 MW per 2 meters. Since experiments at LLNL have demonstrated that RK traveling-wave structures (TWS's) are capable of producing the desired high-power microwave pulses, 200 MW per output with 420 A average current [3], and there is no major difficulty in achieving 360 MW per output with 600 A average current [6], therefore, we can put one RK structure every 2 meters to meet the power requirement. Previous studies have indicated that the total number of extraction cavities the drive beam can be transported through in a RK-TBA is mainly determined by the beam break-up (BBU) factor [4,9]. In a recent study it has been shown that with the introduction of the "betatron node" scheme combined with De-Q-ing technique controllable BBU may be achieved for RK extraction cavities as many as 150 [12]. If we have a total of 150 such RK structures in one unit of TBA (300 m long) and we use 10 MeV, 600 A drive beam and 300 KV/m reacceleration gradient the beam to rf efficiency of such a system is calculated to be around 90% [12].

Table 1. Some latest parameters for SLAC's concept of the
1 TeV linear collider

RF frequency of main linac (GHz)	11.4
Accelerating gradient (unloaded) (MV/m)	100
Pulse length (ns)	250
Section length L (m)	1.8
RF power per section (MW)	350

Longitudinal dynamics of the drive beam is among the important issues for the demonstration of technical feasibility of the RK-TBA concept. In the present scheme, the drive beam is required to stay bunched longitudinally over 150 extraction cavities. Space charge effects cause initially tight bunches to expand. The debunching process is further aggravated by the energy spreads along the beam bunches as they interact with rf fields. In usual traveling wave extraction cavities, rf waves are in synchronism with the drive beam and debunching becomes very severe after a few cavities. Beam debunching, if uncompensated, will result in reduced power extraction in subsequent cavities, as is shown in Figure 3. To overcome this problem, we employ a scheme in
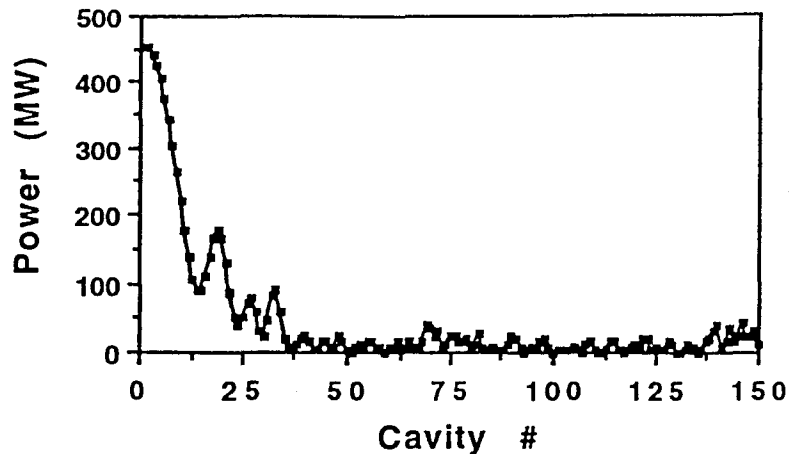
Fig. 3. Simulation result of power extraction versus cavity number for 3-cell traveling wave structures in which the field ($2\pi/3$ mode) is in synchronism with the drive beam (operating frequency 11.424 GHz, cavity group velocity 0.28 c, beam energy 10 MeV and average beam current 600 A.)

which the drive beam is off synchronism with the operating wave mode; more specifically, the phase velocity of the rf field is larger than the speed of light, c, so that the particle bunches always lag behind the decelerating wave and the energy loss becomes phase dependent, as illustrated in Figure 4. This is what we call the "inductive detuning" scheme and it can effectively bunch the beam. The concept of the inductive detuning is actually well known for standing wave structures (SWS's), e.g., the "penultimate" cavity in a klystron, in which the frequency of the cavity is detuned away from the resonant frequency [2]. For the TWS's of RK-TBA, the approach we take is to keep the frequency ω of the operating mode unchanged, but reduce its wave number k, such that wave field advances faster than the beam. In this case particles at the front of the beam bunch lose more energy (due to their interaction with stronger wave field) and slow down, while particles at the tail of the bunch lose less energy, and will therefore, "catch up". This mechanism causes a continuous "sharpening" of the beam bunch, thus counteracting the debunching forces.
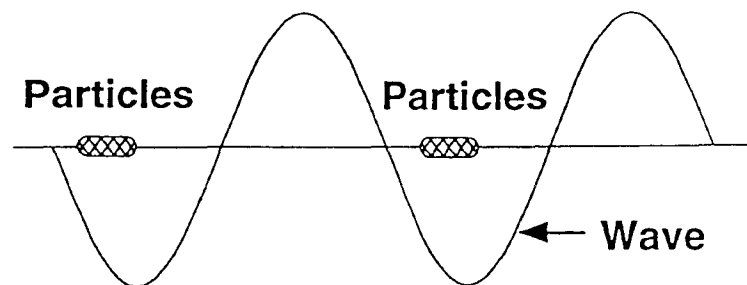

Fig. 4. Schematic of the "inductive detuning" concept

4

The resulting longitudinal phase space continues to rotate in a stable "rf bucket" with a relatively stable bunch length. In this way, stable power extraction and beam bunching can be achieved simultaneously over many cavities.

As mentioned above, the extraction cavities used in the RK-TBA are TWS's. They are favored over the SWS's because of their reduced electrical surface field stress [2]. A typical TWS consists of multiple cells with the last one being, normally, the output cell (see Fig.1). A computer code named "RKS" has, previously, been developed by Ryne and Yu for theoretical investigation of using TWS's to extract power from RK's [14]. Inorder to use the RKS code to study the inductive detuning cases, we have recently derived a more general theoretical framework [15] based on a previous analytic work by Ryne and Yu [16]. The new theory applies to the non-synchronism cases as well as the synchronism case.

This study concerns itself with the longitudinal dynamics of a 360-m long RK-TBA unit (Fig. 2). We carried out extensive investigations on how to employ the inductive detuning scheme on RK-TWS's to achieve power extraction and beam bunching at the same time, and we also examined several other related issues. In section 2, we first briefly describe the "RKS' code, and then present two main analytic formulas obtained in our recently developed theory for using inductively detuned TWS's to extract power from RK's. In section 3, we present our simulation results on the "inductive detuning" scheme and demonstrate that with appropriate detuning angle(s) the output power can be maintained stably for 150 extraction cavities across one RK-TBA unit. In sections 4 and 5, we present, respectively, our simulation studies on the "adiabatic capture" scheme and the chopper operation and show that an initial uniform beam, of 2.5 to 5 MeV and of 1.5 kA (or less) which comes out of the injector, can be manipulated into a bunched beam of 10 MeV and 600 A (average current) with the required microbunch length for stable propagation in the main RK-TBA. In section 6, we examine the "after-burner" scheme and show that the electron beam that exits the main TBA can continue to drive at least another 12 cavities, and therefore, can further enhance the beam to rf efficiency and also make the disposal of the beam easier. A summary is given in section 7.

2. RKS Code and Main Analytic Formulas For Inductively Detuned TWS's

2.1. RKS Code

The computer code used in our numerical simulations is called "RKS". It was previously developed by Ryne and Yu [14] for studying the interaction of a charged particle beam with an electromagnetic wave in a relativistic klystron. The code solves self-consistently the single particle equations of motion for the beam and the coupled circuit equations that govern cavity excitation and it includes the calculation of the space charge effect. It assumes a single dominant mode and cylindrical symmetry of its fields inside the cavity. The code has been checked against the relativistic klystron experiments conducted by the Microwave Source Facility group at LLNL [14] and has also been employed to assist in the design of the reacceleration experiment [7]. These studies have shown that results from the code are consistent with experimental results [10,14].

2.2 Main Formulas For Inductively Detuned TWS's

To carry out simulation study on a TWS with the RKS code we need a so called "matching condition(s)" to determine the eigenfrequency and the external quality factor for the output cell of the TWS. This matching condition, once satisfied, will guarantee that the TWS propagates and amplifies only a forward traveling wave and there exists no backward wave. Previously, a formula for the matching condition was obtained in an analytic theory by Ryne and Yu [16], however, it applies only to the synchronism case when the beam and the field are in phase. Inorder to use the RKS code to study the inductive detuning cases, we have recently derived a more general theoretical framework [15] based on the previous work and obtained a matching condition formula which applies for the non-synchronism cases as well as the synchronism case. The formula is given as follows

$$
\begin{aligned}
\omega_N &= \omega_v - \frac{V_g}{2L_p \cdot \sin(\alpha)} \left[\frac{\sin(N+1)\Delta^-/2}{\sin(N\Delta^-/2)} \cdot \cos \Delta^+/2 \right] \\
(Q_N)^{-1} &= \frac{V_g}{\omega_N L_p \cdot \sin(\alpha)} \left[\frac{\sin(N+1)\Delta^-/2}{\sin(N\Delta^-/2)} \cdot \sin(\Delta^+/2) \right]
\end{aligned}
\tag{1}
$$

where ω_N and Q_N denote, respectively, the eigenfrequency and the external quality factor of the last cell (output cell) of a N-cell TWS. ω_v denote the eigenfrequencies of the other N-1 cells in

the TWS, which are assumed to be identical. L_p and V_g denote, respectively, the longitudinal dimension and the group velocity of a single cell. Also α and α' are, respectively, the phase advances of the wave field and the beam across one cell. In (1) we also have $\Delta^{\pm} = \alpha' \pm \alpha$ with Δ^- being defined as the so called detuning angle. Then $\Delta^- = 0$ corresponds to the synchronism case, while $\Delta^- \neq 0$ corresponds to the non-synchronism cases and in particular $\Delta^- > 0$ corresponds to the inductive detuning cases when the wave travels faster than the beam.

It has also been derived in our theory a formula that quantifies the power extraction from the output cell of a N-cell TWS. The formula may be expressed as follows

$$P_{out} = \Gamma(\Delta^-) \cdot \{\frac{(I_{ind})^2}{4}(\frac{\omega L_p}{V_g})[(\frac{R}{Q})/2] \cdot N(N + 1)\} \tag{2}$$

where I_{ind} and R/Q denotes, respectively, the induced current and the shunt impedance of the structure. The coefficient $\Gamma(\Delta^-)$ is a function of the detuning angle Δ^- and it can be determined from numerical simulation(s) using the RKS code. Eq. (2) relates the power output P_{out} to the induced current, the detuning angle and also cavity parameters, and therefore, it is useful for cavity design. The specific cavity structure that meets the requirements can be designed with the *URMEL* [17] and the *MAFIA* codes [18].

In the following we present the results of our RKS simulation study on the "inductive detuning scheme" and several other issues related to the longitudinal dynamics of the drive beam in a 1 TeV RK-TBA.

3. RK-TBA With Inductively Detuned TWS's

Figure 5 presents the output power from each of 150 TWS's in the main TBA section for both a successful inductive detuning case and its corresponding synchronism case. The parameters for the inductive detuning case are given in Table 2. It is seen in Fig. 5 that for the synchronism case the level of the extracted power P_{out}, declines sharply due to the space charge debunching effect as the drive beam traverses the RK-TBA. In contrast, when the TWS's are properly detuned, the rf bucket can be maintained stably and output power can be sustained at the desired level (~360 MW) for all the 150 extraction cavities. The physical mechanism of the inductive detuning effect can be explained as follows: In a TWS that is inductively detuned, the field advances faster than the beam, therefore, particles at the front of the beam bunch lose more energy and slow down,
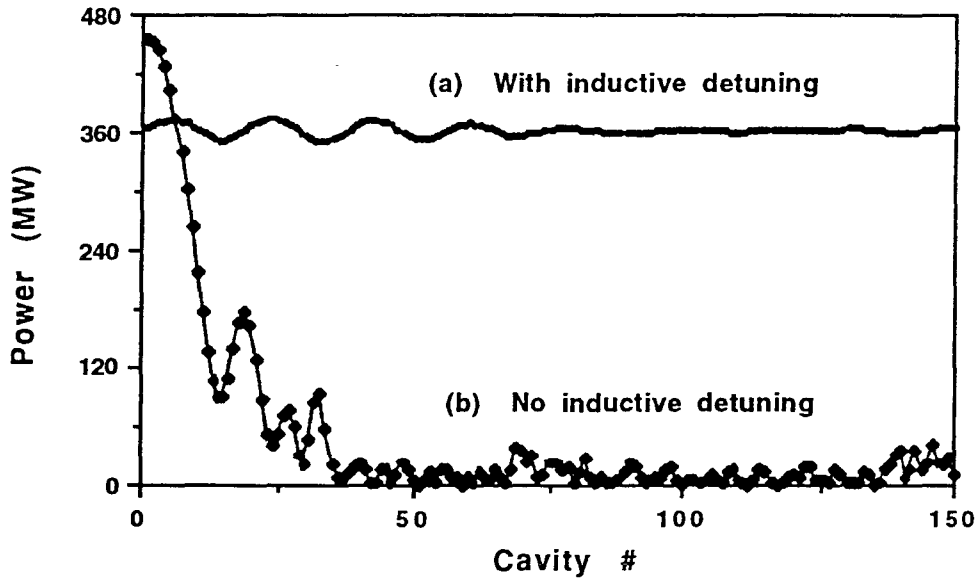
Fig. 5. Power extraction from 150-cavities in one unit of RK-TBA: (a) with inductive detuning ($\Delta^- = 30°$, phase velocity 1.33c); (b) no inductive detuning ($\Delta^- = 0°$, phase velocity 1.0c).

Table 2. Parameters related to the inductive detuning case

Drive frequency	11.424 GHz
Operating Mode	TM_{010}
Phase shift per cell	90°
Wave length	2.626 cm
Phase velocity	1.33 c
Number of cells	3
Group velocity	0.28 c
Shunt impedence per cell (R/Q)	13.5 (Ω)
Eigen frequency for the first 2 cells	11.424 GHz
Eigen frequency for the 3rd cell	11.666 GHz
Wall-dissipation quality factor	7000
External quality factor for the 3rd cell	6.5
Aperture inner radius	8 mm
Aperture outer radius	12.5 mm
Iris thickness	2.5 mm
Longitudinal dimension of each cell	8.754 mm
Beam energy	10 MeV
Beam current (average)	600 A
Bunch length	0.51 cm
Beam radius (rms)	2.5 mm

8

while particles at the tail of the bunch lose less energy, and will "catch up". This causes a continuous "sharpening" of the beam bunch, thus counteracting the debunching forces from the space charge. The resulting longitudinal phase space continues to rotate in a stable "beam bucket" with a relatively stable bunch length (the small fluctuation on the power level is due to this "synchrotron motion" of a rotating "beam bucket"). In this way, the stable power extraction and beam bunching can be achieved simultaneously over many cavities.

The synchronism case in Fig. 5 consists of conventional 3-cell TWS's operating at TM_{010} mode that has $2\pi/3$ phase advance per cell. In the inductively detuned case the operating detuning angle is 30°, the cavity is therefore operating at a TM_{010} mode that has $\pi/2$ phase advance per cell. The longitudinal dimension of each cell is the same in the two cases [5] while the transverse dimensions are varied. *URMEL* and *MAFIA* codes were used for detailed cavity design [19]. Cavity parameters listed in Table 2 were obtained from these code studies.

Figures 6(a) and 6(b) are the longitudinal phase distribution of a beam bucket for the inductive detuning case in Fig. 5, respectively, just before the 1st TWS and after the 110th TWS. It is seen that after 110 extraction cavities the beam bucket maintains the initial bunch length, ~ 70° (the wave length is measured as 360°). It is also noted that the bucket has a large energy spread, $10 \sim 15\%$. This energy spread provides strong Landau damping and drastically reduces the beam break-up (BBU) instability in the induction machine of the RK-TBA. This issue is discussed by Houck, et al in a separate study [19].
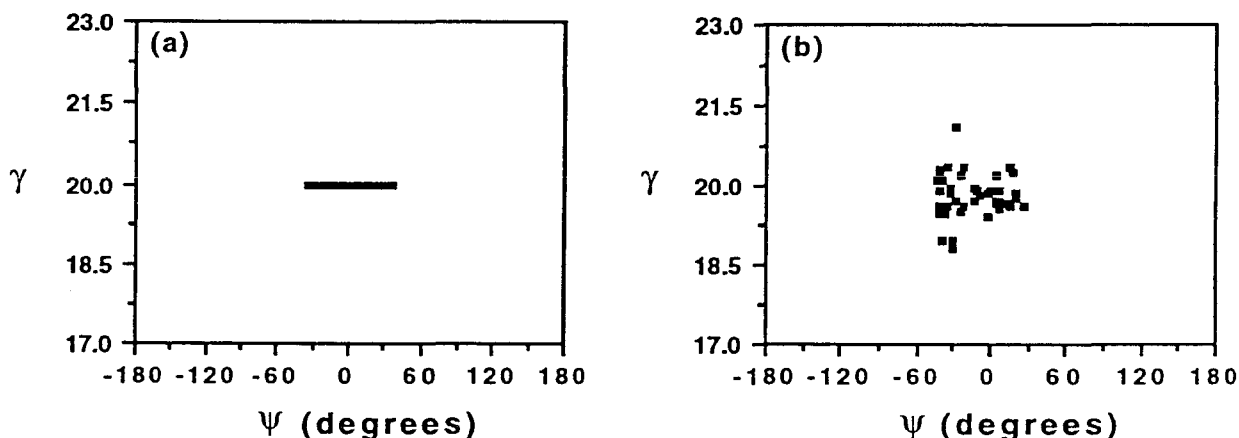

Fig. 6. Phase distribution of a beam bucket for the inductive detuning case in Fig. 5: (a) Just before the 1st TWS; (b) after the 110th TWS and 2 m reacceleration.

A key feature for RK-TBA design is the cavity filling time, i.e., the time it takes for rf field in a cavity to reach equilibrium state. In Figure 7 we present the time dependences of output power

A key feature for RK-TBA design is the cavity filling time, i.e., the time it takes for rf field in a cavity to reach equilibrium state. In Figure 7 we present the time dependences of output power
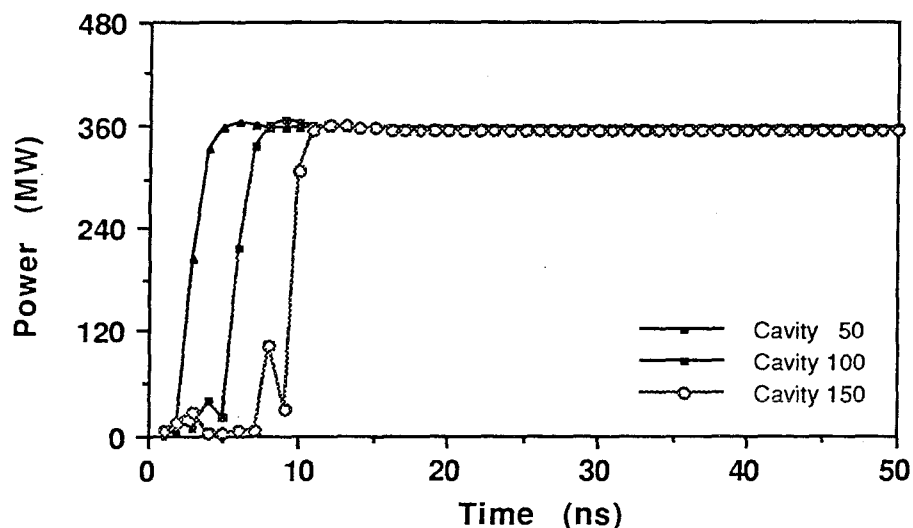

Fig. 7. Time evolutions of output power at 50th, 100th and 150th TWSs for the non-synchronism case in Fig. 5.

at the 50th, 100th and 150th extraction cavities for the inductive detuning case in Fig. 5. It shows that after about 15 ns the fields in all the cavities reach their equilibrium states. This indicates that the erosion on the beam head due to cavity filling process is not serious. The short fill time is a result of low Q and high V_g.

Further RKS simulation studies were conducted to examine the sensitivities of the inductive detuning scheme to two important parameters: the bunch length and the detuning angle:

(i) With respect to the bunch length

Figures 8(a) and 8(b) show power extraction from 150 cavities that are 30° detuned with the bunch length 50° and 90°, respectively. It is seen that for the 30° detuning angle the effective bunch length can be fairly flexible, although when the bunch length is beyond 90° the results start to deteriorate.

(ii) With respect to the inductive detuning angle

To sustain the level of output power throughout the main TBA section the extraction cavities need to have enough detuning. Figures 9(a) and 9(b) show power extraction from 150 cavities that are, respectively, 35° and 25° detuned. It is seen that when the detuning angle is above 30° the result is similar to that of the 30° detuning case, but when the detuning angle is somewhat

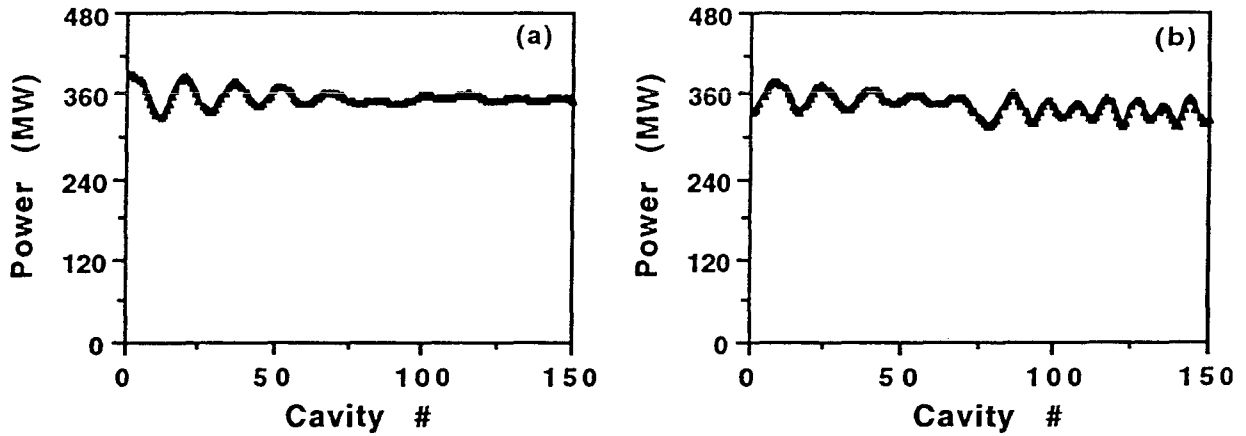bellow 30°, e.g. at 25°, the cavities are unable to sustain the level of output power throughout the whole 150 TWS's.

Fig. 8. Power extraction from 150 cavities that are 30° detuned: (a) 50° bunch length; (b) 90° bunch length.
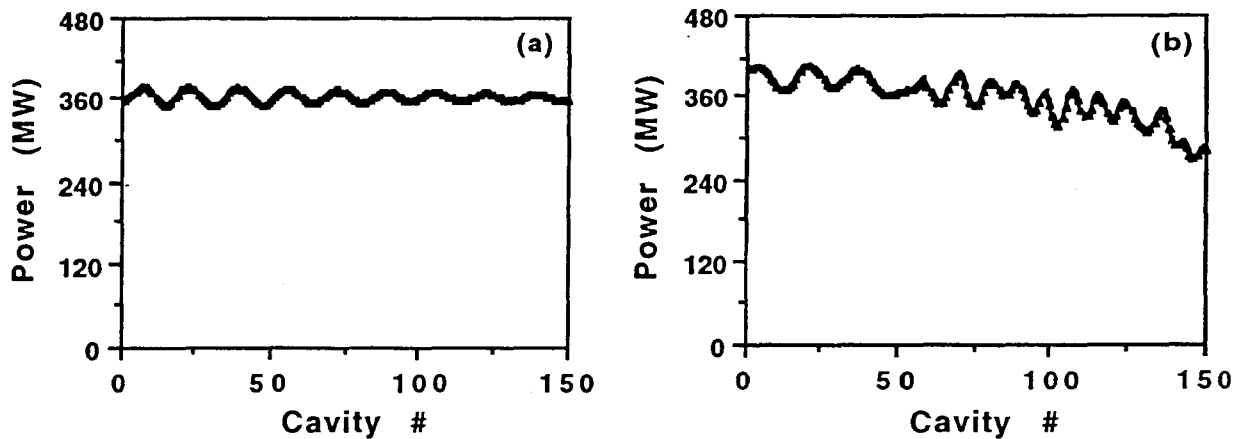
Fig. 9. Power extraction from 150 cavities driven by a beam of 70° bunch length: (a) 35° cavity detuning angle; (b) 25° cavity detuning angle.

4. "Adiabatic Capture"

As it is learnt from Section 3, the desired bunch length for the drive beam of the main TBA section is about 1/5 of the distance between adjacent bunches. Such a train of beam bunches could, of course, be generated in a straightforward way by chopping a continuous beam with a chopper as will be discussed in Section 5, however, that would mean that as much as 4/5 of the beam will be lost, which is not desired as we want to minimize this portion for the efficiency

consideration. For the same reason we also favor the beam to have relatively low energy before it goes through the chopper. But, on the other hand, the main TBA section requires the beam to have certain bunch length and energy. To bridge the gap we have a section called "adiabatic capture". It consists of several "idler" cavities (cavities with large detuning angles) that are properly spaced and induction cells that are placed along the drift tubes between adjacent "idler cavities". A schematic of the "adiabatic capture" section is given in Figure 11. In this section a low energy and long bunches beam is bunched by the "idler" cavities and accelerated by the induction cells to evolve eventually into a beam of bunches with desired energy and bunch length for stable propagation in the main RK-TBA.
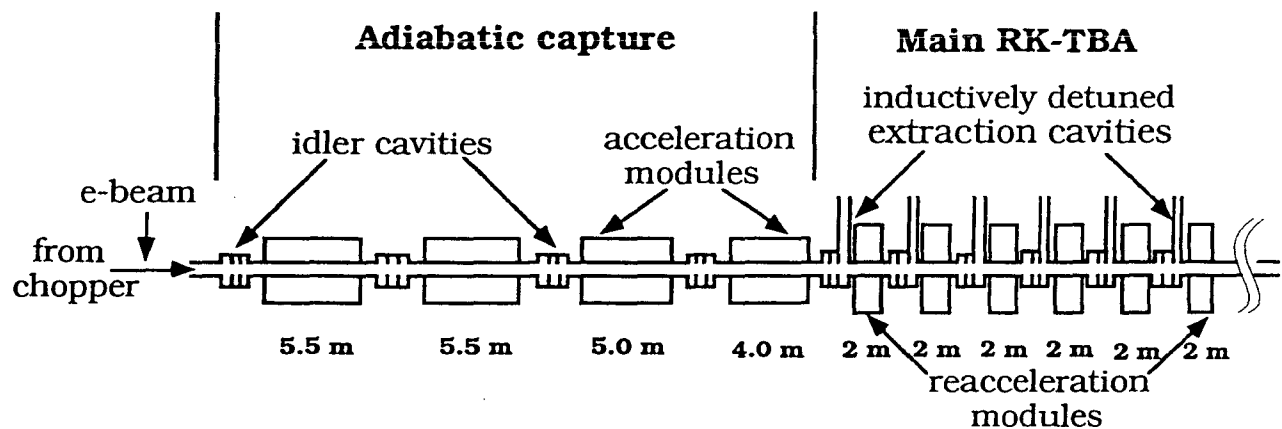

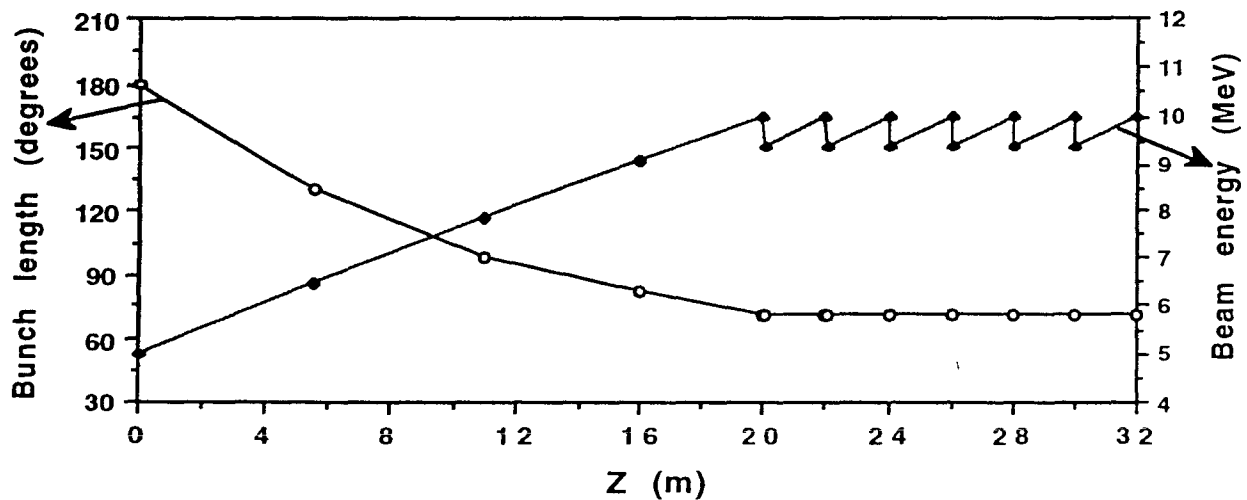Fig. 11. Schematic of "adiabatic capture" scheme

Fig. 12. Evolutions of length and energy of a beam bunch during the "adiabatic capture" process illustrated in Fig. 11.

12

4.1. 5 MeV and 180° bunch length

Figure 12 presents the evolutions of bunch length and kinetic energy of a beam bunch, that starts with 5 MeV kinetic energy and 180° bunch length, through a 20 m "adiabatic capture" section into finally desired 10 MeV energy and 70° bunch length. Figures 13(a) and 13(b) are, respectively, phase distribution of the bunch before and after the adiabatic capture. It is noted that the bunched beam has about 10% energy spread which is consistent with the equilibrium rf bucket in the main TBA section (refer to Fig. 6(b)). The main parameters associated with this process are given in Table 3.1. In Table 3.1, L denotes the distance from the 1st cavity, $\Delta\Phi$ denotes the bunch length in degrees (360° corresponds to one full wave length $\lambda = 2.63$ cm) and E_k denotes the kinetic energy of the beam. All the "idler cavities" used are 3-cell TWS's with 60° inductive detuning.
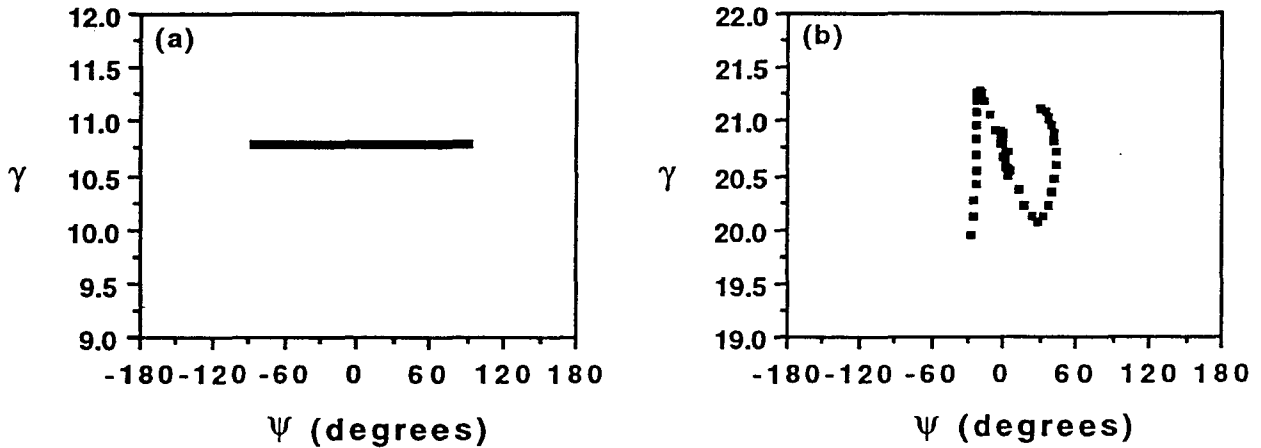

Fig. 13. Phase space distribution of the beam bunch in Fig. 12: (a) before the "adiabatic capture" process; (b) after the "adiabatic capture" process.

Table 3.1. Some Parameters for "Adiabatic Capture" (5 MeV)

TWS #	V_g (c)	L (m)	$\Delta\Phi$ (°)	E_k (MeV)
1	0.20	4.5	140.7	6.22
2	0.20	9.5	104.5	7.51
3	0.20	13.5	85.2	8.47
4	0.20	19.5	70.4	10.02

4.2. 2.5 MeV and 240° bunch length

The efficiency of the RK-TBA could be further increased by starting from a lower energy and less chopped beam. In Figure 14 we present the simulation results of evolutions of length and energy of a beam bunch from initial 2.5 MeV kinetic energy and 240° bunch length to the final 10 MeV energy and 70° bunch length. The main parameters associated with this process are given in Table 3.2. All the "idler cavities" used are 3-cell TWS's with 70° inductive detuning.
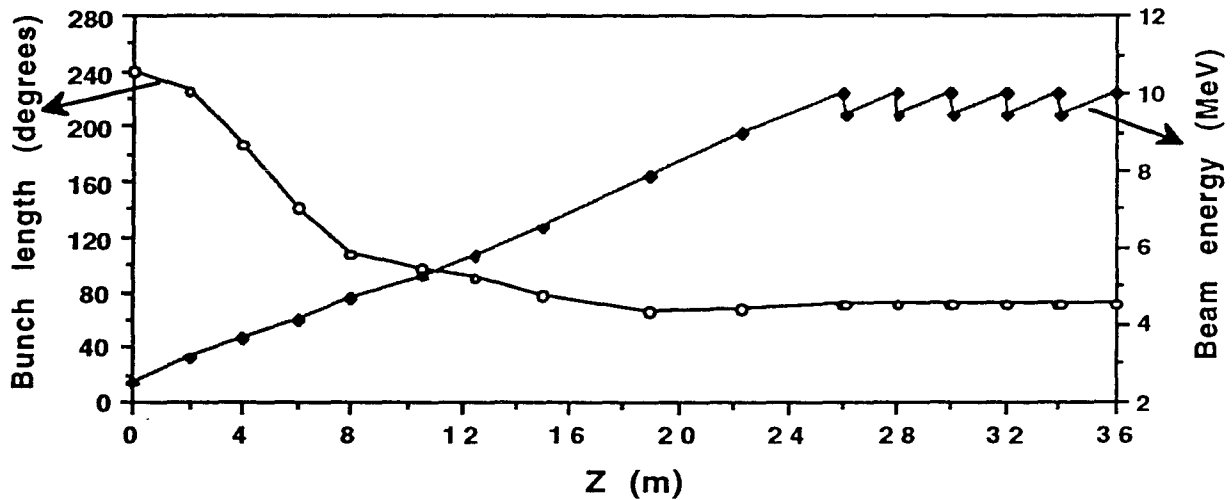

Fig. 14. Evolutions of length and energy of a beam bunch during the "adiabatic capture" process

Table 3.2 Some Parameters for "Adiabatic Capture" (2.5 MeV)

TWS #	V_g (c)	L (m)	$\Delta\Phi$ (°)	E_k (MeV)
1	0.20	2.0	226.0	3.12
2	0.20	4.0	187.0	3.63
3	0.20	6.0	140.9	4.14
4	0.18	8.0	106.8	4.70
5	0.18	10.5	97.7	5.26
6	0.16	12.5	89.8	5.77
7	0.16	15.0	78.1	6.49
8	0.15	19.0	65.7	8.43
9	0.14	22.5	66.3	8.94
10	0.14	26.0	70.0	10.00

14

5. The Chopper

As has been mentioned in Section 4, in our RK-TBA design, after the drive beam comes out of the injector it needs first to go through a chopper to generate a train of beam bunches of certain bunch length before entering the "adiabatic capture" section to acquire further bunching and acceleration. A layout of the original Choppertron made by Haimson Research Corporation [20] and used by the LLNL Microwave Source Facility group [5] is shown in Figure 15. The modulator of the Choppertron is a 5.7 GHz chopping system designed to produce a train of beam bunches with a period corresponding to 11.4 GHz from an initial uniform beam.
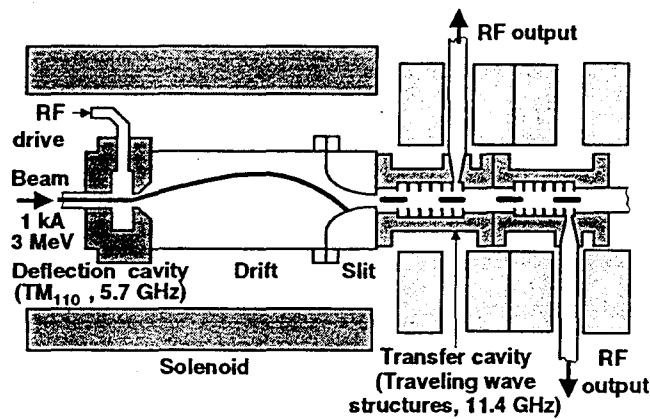
Fig. 15. Layout of the original Choppertron used at LLNL.

The chopper operation is simulated with the 2-1/2 D RKS code and the phase distribution of a beam bunch that comes out of the chopper is given in Figure 16. In this case, the initial electron
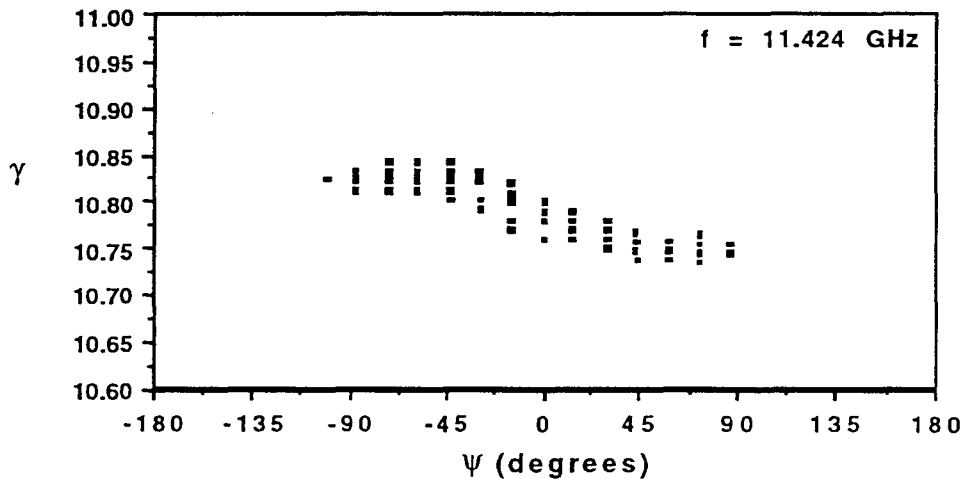
Fig. 16. Phase space distribution of a bunched beam which comes from a chopper chopped initially uniform beam.
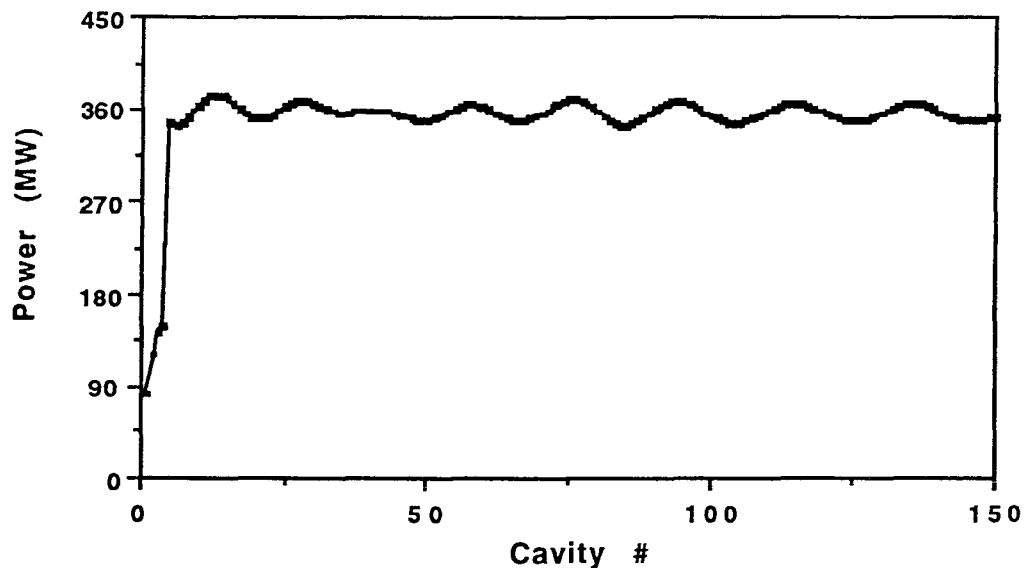
15

Fig. 17. Evolution of output power from the adiabatic capture section to the main TBA section with the beam bucket in Fig. 15 as initial beam bunches

beam is a DC beam of 5 MeV energy and 1.5 KA current, and it has no energy spread. With 0.2 MW rf drive power for the dipole field (TM_{110}) in the deflection cavity we obtain bunched beam of 600 A (average current) coming out of the chopper with each bunch spanning its length about 180° for the 11.4 GHz wave (some "cleaning" on the head and tail of the bunch may be needed). As we can see from Fig. 16 the phase space of the beam bunch has a small but finite energy spread. Although this phase distribution is overall fairly flat it does have some non-uniform features. We then used this more realistic distribution of the beam bunch as the initial condition for the RKS simulations and re-examined the corresponding "adiabatic capture" process and the main Rk-TBA transport. Figure 17 presents the rf power from each of TWS's across the "adiabatic capture" section and the main TBA section. It shows that the level of the output power sustains at 360 MW throughout the entire main TBA section with fluctuation less than 8.5%. The parameters of the cavities used in the "adiabatic capture" section and the main TBA section are the same as those given, respectively, in Section 3 and Section 4.1.

6. After-burner

The electron beam that comes out of the main RK-TBA is still a beam with about 9.4 MeV kinetic energy and 600 A average current. To make the most use of this amount of energy, and to further enhance the beam to rf efficiency, we have another section called the "after-burner" which

16

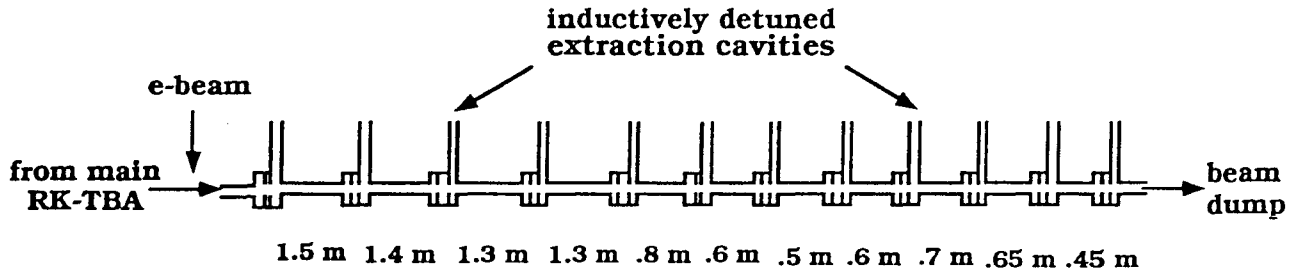**1.5 m 1.4 m 1.3 m 1.3 m .8 m .6 m .5 m .6 m .7 m .65 m .45 m**

Fig. 18 Schematic of "after-burner" section

consists of a dozen or so TWS's that are just like or similar to those used in the main TBA. A schematic of this section is given in Figure 18. In the "after-burner" section the cavities are designed and arranged in such a way that each of them also takes out about 360 MW power from the beam. As for a single period, compared to the main TBA section, in the "after-burner" section: (1) there is no reacceleration, and (2) the distance between two adjacent cavities is adjustable so that the cavities can be placed at positions where the rf current (I_{ind} in Eq. (2)) of the drive beam is relatively stable (about the same as it is in the main TBA section). In addition to the efficiency enhancement, another benefit of the "after-burner" scheme is that it lowers the final energy of the beam considerably, which makes the disposal of the spent beam much easier.

We have carried out RKS simulation on the "after-burner" section in which 12 TWS's with $30°$ detuning are properly arranged (Fig. 18), and the drive beam consists of bunches of $70°$ bunch length and 15% energy spread. The results and some related parameters are given in Table 4. As we can see in Table 4 with the proper choices of the group velocities (V_g) and the spacing (L_s) each of the cavities is able to extract about 360 MW from the beam and the final energy of the beam is around 2.2 MeV. This means a 77.% beam to rf efficiency, $\eta_{b->rf}$, for this section, and therefore, a increase of the whole system $\eta_{b->rf}$ from 84% to 90% or from 88% to 95%, depending on whether the beam bunches at the exit of the chopper is (i) 5 MeV and $180°$ (Section 4.1) or (ii) 2.5 MeV and $240°$ (Section 4.2). To explain how the above $\eta_{b->rf}$ figures were obtained, a brief calculation for case (i) is given as follows:

$$\eta_{b->rf} = \text{Total rf output power / Total input power carried by the beam}$$
$$= [150 \times 360.\ \text{MW} + 12 \times 360.\ \text{MW}] /$$
$$[5\ \text{MV} \times 1500\ \text{A} + (10 - 5)\ \text{MV} \times 600\ \text{A} + 150 \times 360.\ \text{MW}]$$
$$= 90.4\ \%.$$

(In the above calculation, the two terms in the numerator is easy to understand; in the denominator the first two terms correspond, respectively, to the power the beam acquires at the

17

Table 4. Some Parameters for "After-Burner"

TWS #	V_g (c)	L_s (m)*	P_{out} (MW)	E_k (MeV)
1	0.28		363.	8.80
2	0.28	1.50	365.	8.19
3	0.28	1.40	365.	7.58
4	0.28	1.30	362.	6.98
5	0.27	1.30	366.	6.37
6	0.27	0.80	357.	5.77
7	0.26	0.60	362.	5.17
8	0.26	0.50	355.	4.58
9	0.25	0.60	361.	3.98
10	0.24	0.70	361.	3.37
11	0.22	0.65	369.	2.76
12	0.22	0.45	358.	2.16

* Distance from the last cavity.

injector section and at the adiabatic capture section, while the third term corresponds to the total power the beam obtains from the induction machine during the 150 reacceleration processes.) Figure 19 shows the phase distribution of a beam bunch in the above "after-burner" section: (a)
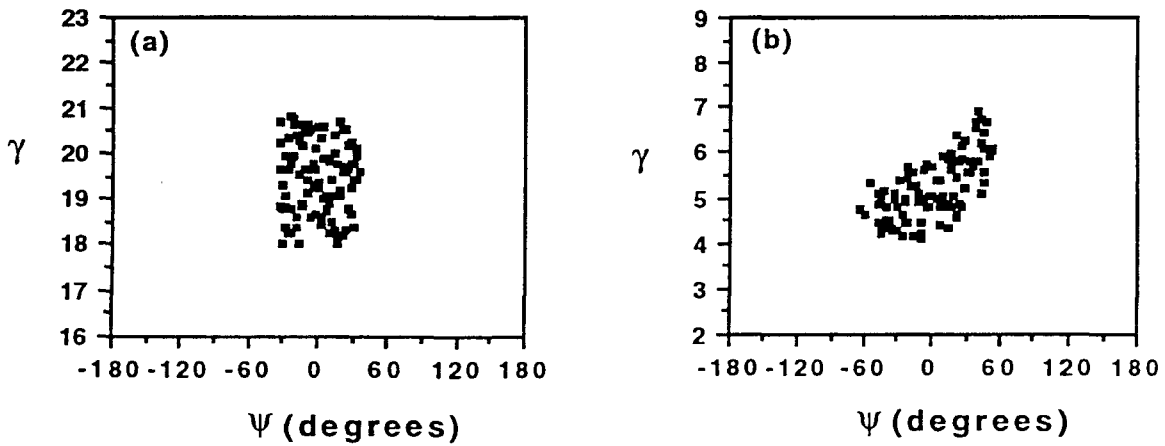

Fig. 19. Phase distribution of a beam bunch in the "after-burner" section: (a) before the 1st cavity; (b) after the 12th cavity

18

before the 1st cavity; (b) after the last cavity. As we can see from Fig. 19(b) that even at the end of the "after-burner" section the beam bunch is still well preserved in the phase space.

7. Summary

We are carrying out a design study on the longitudinal dynamics of a 1 TeV relativistic klystron two-beam accelerator (RK-TBA) which is being proposed as a possible next linear collider. We employed the "inductive detuning" concept as a way to contain space charge debunching effect on the drive beam and have demonstrated with simulations the stable power output at desired level for 150 extraction cavities in the RK-TBA. We carried out simulation study to explore schemes that can "adiabatic capture" an initial low energy and long length beam bunch to a final desired high energy and tight beam bunch for stable propagation in the main RK-TBA. We included chopper in our simulation study and again obtained the successful case with the output power being relatively stable across the entire main TBA section. We also examined the "after-burner" scheme and obtained optimum parameters that can further enhance beam to rf conversion. In the future we will carry out full 2-1/2 D RKS simulations and investigate the transverse focusing issue.

Acknowledgments

References

[1] A. M. Sessler and S. S. Yu, Phys. Rev. Lett. 58 (1987) 2439.

[2] M. A. Allen, et al, Phys. Rev. Lett. 63 (1989) 2472.

[3] T. L. Houck, D. Rogers, R. D. Ryne and G. A. Westenskow, "Relativistic Klystron Research for Two-Beam Accelerator," SPIE Symposium on Intense Microwave and Particle Beams II Proceedings Vol. 1629-1647 (1992).

[4] G. A. Westenskow, et. al., "Transverse Instabilities in a Relativistic Klystron Two-Beam Accelerator", Proc. 16th Int'l LINAC Conf., Aug, 1992, pp.263-267.

[5] T. L. Houck and G. A. Westenskow, "Status of the Choppertron Experiments," Proc. 16th Int'l LINAC Conf., Aug , 1992, pp. 498-500.

[6] T. L. Houck and G. A. Westenskow, "Status of an Induction Accelerator Driven, High-Power Microwave Generator at Livermore," Proc. Intense Microwave Pulses, ed. by H. E. Brandt, SPIE 1872-16 (1993).

[7] G. M. Fiorentini, T. L. Houck and C. Wang, Proc. Intense Microwave Pulses, ed. by H. E. Brandt, SPIE 1872-17(1993).

[8] G. A. Westenskow and T.L. Houck, "Reacceleration Experiment to Demonstrate the Concept of Efficiency Enhancement in a Relativistic Klystron Two-Beam Accelerator", Proc. PAC (1993) 2611.

[9] T. H. Houck, "Design Study of a Microwave Driver for a Relativistic Klystron Two-Beam Accelerator", Proc. PAC (1993) 2590.

[10] T.L. Houck and G.A. Westenskow, "Status of Experiments at LLNL on High-Power X-band Microwave Generators," Proc. Intense Microwave Pulses, ed. by H. E. Brandt, SPIE 2154 (1994) 84.

[11] H. Li, T. L. Houck, S. Yu and N. Goffeney, Proc. Intense Microwave Pulses II, ed. by H. E. Brandt, SPIE 2154 (1994) 91.

[12] S. Yu, F. Deadrick, N. Goffeney, E. Henestroza, T. Houck, H. Li, C. Peters, L. Reginato, A. Sessler, D. Vanecek and G. Westenskow, "Relativistic-Klystron Two-Beam-Accelerator As A Power Source For A 1 TeV Next Linear Collider -- A Systems Study", Presented at 17th Int'l LINAC Conf., Japan, August 22-26, 1994, to be published in the Proceedings.

[13] "NLC, Test Accelerator, Conceptual Design Report", Stanford Linear Accelerator Center, Stanford, CA, SLAC-Report-411, August, 1993.

[14] R. Ryne and S. S. Yu, Proc. 15th Int'l LINAC Conf., LA-12004-C (1990) 180.

[15] H. Li, S. S. Yu and A. Sessler, "Theory for Inductively Detuned Traveling Wave Structures", to be submitted to Phys. Rev. E for publication.

[16] R. Ryne and S. S. Yu, Proc. 15th Int'l LINAC Conf., LA-12004-C (1990) 177.

[17] T. Weiland, Nuclear Instruments and Methods 216 (1983) 329.

[18] F. Ebeling, et al, Mafia User Guide, Los Alamos National Laboratory Report LA-UR-90-1307 (1989).

[19] S. Yu, F. Deadrick, N. Goffeney, E. Henestroza, T. Houck, H. Li, C. Peters, L. Reginato, A. Sessler, D. Vanecek and G. Westenskow, "Relativistic Klystron Two-Beam Accelerator As A Power Source For A 1 TeV Next Linear Collider, Conceptual Design Report", LBL, Berkeley, CA, September, 1994.

[20] J. Haimson and B. Mecklenburg, Report No. HRC-774, Haimson Research Corporation, Palo Alto, CA, 1988.